

Ethanol / Oxygene microfluidic biofuel cells.

D. Selloum^{a,b*}, S. Tingry^c

^a Univ. Ouargla, Fac. des Sciences Appliquées, Lab. Dynamique, Interactions et Réactivité des Systèmes, BP 511 Ouargla, Algeria.

^b Laboratoire de Croissance et Caractérisation de Nouveaux Semiconducteurs (LCCNS), Faculté de Technologie, Université de Sétif 1.

^c Institut Européen des Membranes, UMR 5635, ENSCM-UMII-CNRS, place Eugène Bataillon, 34095 Montpellier, France.

ARTICLE INFO

Article history:

Received: 05 June 2018

Revised: 27 June 2018

Accepted: 14 July 2018

Published online: 16 July 2018

Keywords:

Microfluidics

Carbon nanoparticles

Bioelectrodes ;

Enzymatic biofuel cell

ABSTRACT

This work presents the construction of an ethanol microfluidic biofuel cell (MBFC) based on bioelectrodes and operating in a Y-shaped microfluidic channel. At the cathode, the oxygen is reduced by laccase, whereas at the anode, ethanol is oxidized by alcohol dehydrogenase. The enzymes were immobilized in the presence of reactive species at gold electrode surfaces. Oxidant and Fuel streams move in parallel laminar flow without turbulent mixing into a microchannel. The benefit of the carbon nanoparticles with higher surface porosity was explained by the high porous structure that offered a closer proximity to the reactive species and improved diffusion of ethanol and oxygen within the enzyme films. The higher current and power densities were achieved for shorter and wider electrodes that allow for thinner boundary layer depletion at the electrodes surface resulting in efficient catalytic consumption of fuel and oxidant. This miniaturized device generated maximum power density of $90 \mu\text{W cm}^{-2}$ at 0.6 V for a flow rate $16 \mu\text{L min}^{-1}$.

© 2018 mbmscience.com. All rights reserved.

Introduction

Biofuel cells (BFCs) have recently attracted considerable attention for the conversion of chemical energy to electricity through biological catalysts immobilized on electrodes. [1] There are two types of BFCs depending on the nature of the catalyst to perform the redox reactions at the electrodes: enzymatic BFCs work from enzymes [1,3] and microbial BFCs use bacteria[3,4]. These devices are built from the assembly of a bioanode, which oxidizes the fuel substrate, and with a biocathode which reduces the oxidizer. Enzymatic BFCs operate with fuels such as glucose, ethanol, methanol and oxidant as oxygen. An important aspect of the performance and stability of these devices is the density of electrochemically active enzymes on the electrode.

Combination of microfluidic technologies and biological materials (enzymes) has given rise to the development of microfluidic biofuel cells (MBFC) [2-5]. These devices used enzymes as catalysts to convert chemical energy into electricity [6]. The components of MBFC are analogous of the conventional microfluidic fuel cells based on anodic and

cathodic compartments [1,7,8]. Fuel and oxidant streams move in parallel laminar flow without turbulent mixing into a microchannel fabricated using soft lithography methods [9]. These devices operate without the need of a separation membrane allowing for different pHs at the anolyte and the catholyte for optimal kinetics reaction. The mixing of the flows can only occur through diffusion, restricted to a thin interfacial zone in the center of the channel [1, 10].

An important step to construct biofuel cells is the immobilization of enzymes on electrically conductive support. Electrodes modified by enzymes are the subject to develop prospective bioelectrodes to deliver high catalytic current density [11]. However, current densities are limited by low coverage of enzymes on the electrodes, low stability and sluggish electron transfer. The use of conductive nanomaterials with high surface area like carbon nanotubes or nanoparticles for bioelectrode modification provides an alternative and frequently used option to increase enzyme loading [12-13]. The similar dimensions of the particles and the enzymes enable nanomaterials to operate as an electrical wire decreasing electron transfer distance between the electrode and the active site of the enzymes [14]. Besides, their proximity can possibly accelerate the biocatalytic process. These materials

* Corresponding author: Djamel Selloum
E-mail address: selloumdjamel@gmail.com

are attractive for sensing and biosensing applications [15], for efficient bioelectrocatalysis [16] and could have a significant role in the development of biofuel cells. Incorporation of carbon nanoparticle (CNPs) is well-established for electrode surface modification in order to improve electron transfer rate between enzymes and electrode surfaces. One simple method involves encapsulation of carbon nanoparticles in organic [17] or inorganic polymer films [18]. Bioelectrodes based on bilirubin oxidase immobilization have been prepared with phenylsulfonated CNPs by layer-by-layer approach [19-21]. The authors showed that the carbon nanoparticle three-dimensional film electrode promoted mediatorless bioelectrocatalytic oxygen reduction with good efficiency, as the current densities increased with the amount of deposited nanomaterial. Biocomposite CNP-laccase biocathodes have been prepared by entrapment of CNPs within enzyme polymer matrix for O₂ bioelectrocatalysis [22-30].

This paper describes the development of an ethanol MBFC based on bioelectrodes operating in a Y-shaped microfluidic channel to generate maximum power density. At the anode, ethanol was oxidized by alcohol dehydrogenase, whereas at the cathode, the oxygen was reduced by laccase. Electrochemical characterizations of the device were performed by varying the electrode configuration. Electrochemical characterizations is a versatile method with features of simplicity, simple process, cost-efficiency and high quality [31].

Experimental

Materials

Laccase from *Trametes Versicolor* (20 U mg⁻¹ solid), Diaphorase (3-20 U mg⁻¹), Alcohol Dehydrogenase (300 U mg⁻¹), β-nicotinamide adenine dinucleotide sodium salt (NAD⁺), 2-methyl-1,4-naphthoquinone (VK3), Aceton, polyethylenimine (PEI), 2,2'-azino-bis(3-ethylbenzothiazoline-6-sulfonate) diammonium salt (ABTS), Nafion[®] solution (5 wt%), sodium phosphate dibasic dihydrate (Na₂HPO₄·2H₂O) and sodium phosphate monobasic monohydrate (NaH₂PO₄·H₂O) were purchased from Sigma-Aldrich and used without further purification. The phosphate buffer was prepared with Na₂HPO₄·2H₂O and NaH₂PO₄·H₂O (pH 5, 7 or pH 9, 0.1 M). The carbon nanoparticles powder as Super P[®] and KS6 were purchased from TIMCAL.

Bioelectrodes preparation

The biocathode to be employed in the electroreduction of oxygen was prepared by adsorption of enzymes and mediators on the surface of the electrodes by drop casting. 333 μL of laccase (15 mg mL⁻¹) and super-P[®] (15 mg mL⁻¹) in phosphate buffer 0.1M (pH 5) solution was mixed on a vortex mixer. Sequentially, 100 μL of the solution was mixed with ABTS (5.4 mg mL⁻¹) and 10 μL Nafion[®]. Then, 6 μL of the preparation was coated onto Au electrode and left to dry at room temperature before keeping in a low humidity

environment.

The bioanode to be employed in the oxidation of ethanol was prepared by adsorption of successive coatings separated by a dried step at room temperature. 167 μL of ADH (30 mg mL⁻¹) and KS6 (15 mg mL⁻¹) in phosphate buffer 0.1M (pH 7) solution was mixed on a vortex mixer and 6 μL of the preparation was pipetted onto the electrode and dried at room temperature. The same procedure was conducted for the immobilization of NAD⁺ (30 mg mL⁻¹) and then diaphorase (20 mg mL⁻¹). The last coating on the electrode consisted in pipetting 10 μL of VK3 (60 mg mL⁻¹), 190 μL acetone and 10 μL PEI, followed by drying.

Fabrication of the microfluidic cell

The microfluidic chip was fabricated from a standard soft lithography method described elsewhere [32]. Typically, a glass slide was preliminary cleaned, modified sequentially by three photoresist layers (35 μm Etertec HQ-6100) exposed to UV light through a photomask. The structure was then developed by spraying an aqueous solution of sodium carbonate (1 wt%) during 4 min and hardened by a second irradiation. The master was then replicated in PDMS at 70 °C during 2 h. After cooling, the PDMS slab was peeled off from the master and holes were punched using a 1.2 mm diameter tube, to provide an access for Teflon tubing. The PDMS slab was then aligned with an epoxy slide containing electrodes. The device consisted of a Y-shaped channel in PDMS with two inlets and two outlets. The microchannel dimensions were: $L = 3$ cm, $w = 2$ mm and $h = 120$ μm (Fig. 1).

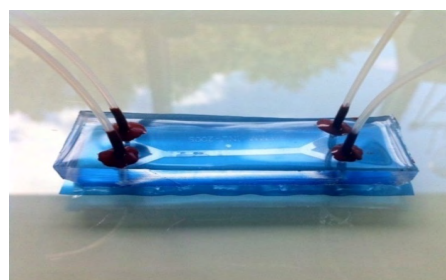


Fig. 1. Photograph of the Y-shaped microfluidic channel in PDMS with two inlets and two outlets.

The PDMS slab was subsequently sealed to an epoxy substrate that accommodated the electrode pattern. The gold electrodes were deposited by sputtering 300 nm thick Au layer on a 10 nm thick Cr adhesion layer on epoxy substrate. Two electrode patterns with different aspect ratio (length-to-width) were studied (Fig. 2): design (A) with electrodes 5 mm long and 1 mm wide; design (B) with electrodes 10 mm long and 0.5 mm wide. The surface of the gold electrodes in contact with the microfluidic channel was 0.05 cm² in both designs.

Electrochemical measurements

The bioelectrodes were characterized separately by polarization curves performed in dioxygen-saturated

phosphate buffer pH 5 0.1 M for the biocathode, or in phosphate solution pH 9, 0.1 M with 160 μL ethanol for the bioanode, after stabilization of the open circuit potential. Electrochemical measurements were performed on a potentiostat Autolab (Eco chemie, Netherlands) at 25°C in phosphate buffer, with a conventional three-electrodes system composed of a stainless steel auxiliary electrode, a calomel saturated reference electrode and the electrode material as working electrode.

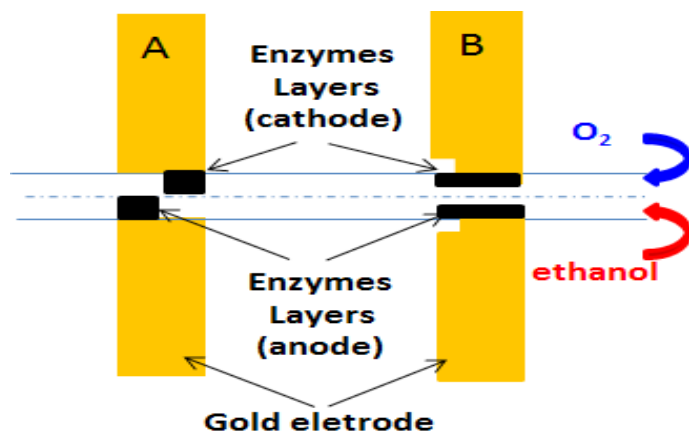


Fig. 2. Photos of gold electrodes ($S=0.05\text{ cm}^2$) confined within a microfluidic channel (120 high and 2 mm wide) and modified by enzyme layers mixed with carbon nanoparticles, design (A): electrodes 5 mm long * 1 mm wide, and design (B): electrodes 10 mm long * 0.5 mm wide.

The MBFC was characterized by the same electrochemical equipment. The cathode was connected to the working electrode, and the counter and reference electrodes were both connected to the anode. The catholyte solution consisted of phosphate buffer solution 0.1 M, pH 5 saturated with O_2 . The anolyte solution contained ethanol 160 μL in phosphate buffer 0.1 M pH 9. Protons diffuse through the liquid–liquid interface created by the contacting streams. The solutions were provided by a syringe pump (Harvad) at variable flow rates and delivered to the cell via tygon tubing.

Results and discussion

The biocathode was evaluated with respect to the bioanode, and a complete MBFC based on a Y-shaped microfluidic channel was tested towards ethanol fuel at room temperature by measuring the optimum power output. To date, only one microchip-based bioanode paired with an external Pt cathode working from ethanol fuel has been developed [36]. This device showed maximal power density of 5 W cm^{-2} at 0.34 V.

A major limitation to obtain high current densities in microfluidic devices is the depletion of fuel and oxidant along the electrode surface, which hinders reaction kinetics and drastically increased the mass transport limitations [37]. Reducing the electrode length can decrease the influence

of the boundary layer depletion and thus improve both the current and power densities [38–41]. As the electrodes design confined in the microchannel is an important element in the manufacture of the microfluidic fuel cells, two different electrode patterns with different aspect ratio (see Fig. 2) were tested to assess their influence on the performance of the MBFC. The total electrode surface and the flow rate were kept constant. Pattern (A) was characterized by electrodes in width that extends over the half of the microchannel, whereas pattern (B) was characterized with narrowed and longer electrodes. It resulted that in pattern (A), the whole solution (anolyte or catholyte) was in contact with the immobilized enzymes while in pattern (B), there was only one part of the solution which showed the immobilized enzymes. Another difference was that in the pattern (A), electrodes are not face-to-face, unlike in pattern (B) and that to avoid contact.

Fig. 3 shows for the different patterns the cell voltage and the resulting power density versus the current density of the ethanol/ O_2 MBFC delivered at the flow rate $16\text{ }\mu\text{L min}^{-1}$. The MBFC was built from an anode based on carbon nanoparticles KS6 and a cathode based on carbon nanoparticles Super P $^{\text{®}}$. The MBFC with electrode pattern (A) shows a semi-plateau and a drop in the potential at high current densities typical of mass transfer limitations, whereas the curve shape for the device with electrode pattern (B) shows important ohmic losses and slower kinetics that in turn diminishes V_{oc} . The position of the electrodes influences the ohmic resistance in the microchannel and accounts, at least in part, to the cell performances: electrodes spaced closed to each other (pattern A) allow low internal resistance, whereas the longer gap between bioelectrodes in pattern (B) increases the pathway that protons need to travel from the bioelectrodes [15].

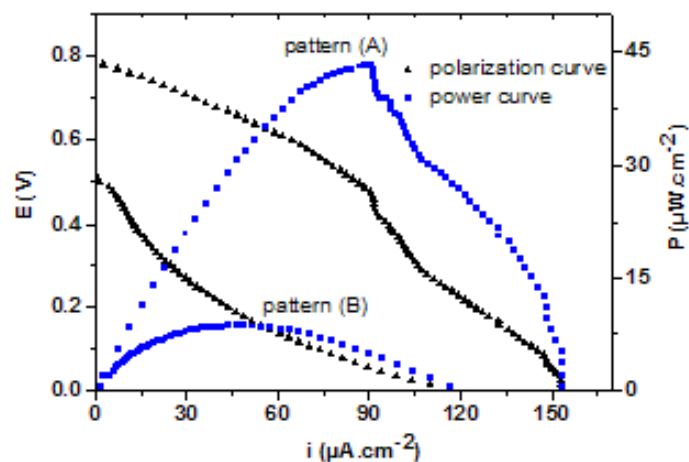


Fig. 3. Polarization (Δ) and power (\square) curves obtained from the ethanol/ O_2 MBFC based on KS6 (anode) and Super P $^{\text{®}}$ (cathode) with electrode patterns (A) and (B), at flow rate $16\text{ }\mu\text{L min}^{-1}$ with anolyte pH 9/catholyte pH 5 in phosphate buffer 0.1M, $v = 3.33\text{ mVs}^{-1}$.

The benefit of the electrode pattern (A) is obvious from biofuel cell performance. The resulting MBFC delivers the highest V_{oc} (0.8 V) and a power density 80% larger than that found with electrode pattern (B) (45 against $10 \mu\text{W cm}^{-2}$). Shorter and wider electrodes result in thinner boundary layers and more efficient catalytic consumption of fuel and oxidant at the surface of the electrodes and thus higher electrode performances. This behavior was also described in the works of Thorson et al. [37] that showed that low aspect ratio (short and wide electrodes) significantly improved the performance of an air-breathing alkaline laminar flow fuel cell. We have therefore chosen the MBFC with pattern (A) for the following work.

The MBFC containing the carbon nanomaterial (fig.4) Super P[®] shows the highest performance increase ($90 \mu\text{W cm}^{-2}$ at 0.6 V) in 2-folds compared to the initial system, supporting a kinetic enhancement of the ethanol oxidation. This result can be attributed to the increased surface area of the anode and therefore to the higher amount of immobilized reactive species on the anode. Besides, the porous structure of the nanoparticles Super P may promote the proximity of the conductive nanoparticles close to the active site of the active species that possibly reduces the electron transfer distance and accelerates the bioelectrocatalytic process, and thus the power density of the MBFC.

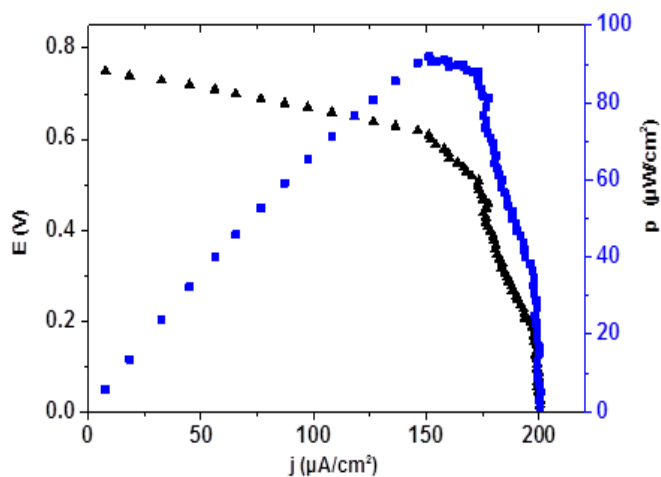


Fig. 4. Polarization (Δ) and power (\square) curves of various MBFCs tested with the electrodes with anolyte pH 9/ catholyte pH 5 in phosphate buffer 0.1M, flow rate = $16 \mu\text{L min}^{-1}$. MBFC built from bioanode with KS6 and biocathode with Super P

The evolution of the power density with time and after keeping the electrode in humid atmosphere one night shows quite stable V_{oc} but a pronounced loss of current densities mainly due to the immobilization procedure that was not sufficiently efficient to prevent the leaching of the cofactor NAD^+ and the mediator ABTS, that contributes to a low stability of the BFC with time. In literature, ethanol-based

biofuel cells based on macro-scale electrodes are working with the NAD^+ cofactor in the solution [43-46]. More works are thus required to get durable and stable MBFCs. Although comparison with the literature is not straightforward, this ethanol/ O_2 BFC delivers a competitive and high power density of $90 \mu\text{W cm}^{-2}$ with reported MBFC based on glucose fuel [29-31] and ethanol fuel for a microchip-based bioanode paired with an external Pt cathode [36].

Conclusion

This work presented an ethanol MBFC based on bioelectrodes operating in a Y-shaped microfluidic channel. We showed the enhancement of bioelectrodes electroactivity by carbon nanoparticles as efficient hosts for redox species. The large surface area and the electronic conductivity of the nanoparticles enhance both the reactive species loading and electron transfer rate to the electrodes. Besides, carbon nanoparticles with higher porous structure increased bioelectrocatalytic processes, by offering a closer proximity between the reactive species and the electrode surface, and by improving diffusion of ethanol and oxygen within the enzyme films.

The ethanol MBFC was optimized as function of electrode patterns with different aspect ratio. Higher current and power densities were achieved for shorter and wider electrodes that allow for thinner boundary layer depletion at the electrodes surface resulting in efficient catalytic consumption of fuel and oxidant.

This miniaturized device, based on bioelectrodes and working from ethanol, generated the highest maximum power density of $90 \mu\text{W cm}^{-2}$ at 0.6 V for a flow rate $16 \mu\text{L min}^{-1}$.

References

1. D. Selloum, S. Tingry, V. Techer, L. Renaud, C. Innocent, A. Zouaoui J. Power Sources 269 (2014) 834-840.
2. D. Selloum, A.A. Chaaya, M. Bechelany, V. Rouessac, P. Miele, S. Tingry, J. m. chemistry A 2 (2014) 2794-2800.
3. L. Renaud, D. Selloum, S. Tingry, J. Microfluidics and Nanofluidics. 18 (2015) 1407-1416.
4. A. Zebda, L. Renaud, M. Cretin, C. Innocent, F. Pichot, R. Ferrigno, S. Tingry, J. Power Sources 193 (2009) 602-606.
5. A. Zebda, L. Renaud, M. Cretin, C. Innocent, R. Ferrigno, S. Tingry, J. Sensors and Actuators B: Chemical 149 (2010) 44-50.
6. F. Davis, S. P. Higson, J. Biosens. Bioelectron. 22 (2007) 1224-1235.
7. R. S. Jayashree, S. K. Yoon, F. R. Brushett, P. O. Lopez-Montesinos, D. Natarajan, L. J. Markoski, P. J. A. Kenis, J. Power Sources 195 (2010) 3569-3578.
8. D. Fuerth, A. Bazylak, J. Fluids Eng. 135 (2013) 021102-021109.
9. E. R. Choban, L. J. Markoski, A. Wieckowski, P. J. A. Kenis, J. Power Sources 128 (2004) 54-60.
10. R. F. Ismagilov, A. D. Stroock, P. J. A. Kenis, G. Whitesides, H. A. Stone, J. Appl. physics Lett. 76 (2000) 2376-2378.
11. E. H. Yu, K. Scott, J. Energies 3 (2010) 23-42.

12. S. D. Minteer, P. Atanassov, H. R. Luckarift, G. R. Johnson, *J. Materials Today* 15 (2012) 166-173.
13. S. Ha, Y. Wee, J. Kim, *J. Top. Catal.* 55 (2012) 1181-1200.
14. M. Opallo, R. Bilewicz, *J. Advances in Physical Chemistry* (2011) 21 pages.
15. X. Luo, A. Morrin, A. J. Killard, M. R. Smyth, *J. Electroanalysis* 19 (2007) 244-252.
16. S. Tsujimura, Y. Kamitaka, K. Kano, *J. Fuel cells* 7 (2007) 463-469.
17. A. M. Zimer, R. Bertholdo, M.T. Grassi, A. J. G. Zarbin, L. H. Mascaro, *J. Electrochem. Comm.* 5 (2003) 983-988.
18. S. M. Macdonald, K. Szot, J. Niedziolka, F. Marken, M. Opallo, *J. Solid State Electrochem.* 12 (2008) 287-293.
19. A. Lesniewski, J. Niedziolka-Jonsson, C. Rizzi, L. Gaillon, J. Rogalski, M. Opallo, *J. Electrochem. Comm.* 12 (2010) 83-85.
20. A. Lesniewski, M. Paszewski, M. Opallo, *J. Electrochem. Comm.* 12 (2010) 435-437.
21. K. Szot, M. Jönsson-Niedziolka, E. Rozniecka, F. Marken, M. Opallo, *J. Electrochimica acta* 89 (2013) 132-138.
22. U. B. Jensen, M. Vagin, O. Koroleva, D. S. Sutherland, F. Besenbacher, E. E. Ferapontova, *J. Electroanal. Chem.* 667 (2012) 11-18.
23. R. Kontani, S. Tsujimura, K. Kano, *J. Bioelectrochem.* 76 (2009) 10-13.
24. M. Masuda, Y. Motoyama, K. Murata, N. Nakamura, H. Ohno, *J. Electroanalysis* 23 (2011) 2297-2301.
25. M. Ammam, J. Fransaer, *J. Biotechnol. Bioeng.* 109 (2012) 1601-1609.
26. L. N. Akers, M. C. Moore, D. S. Minteer, *J. Electrochimica Acta* 50 (2005) 2521-2525.
27. A. Habrioux, K. Servat, S. Tingry, K. B. Kokoh, *J. Electrochem. Comm.* 11 (2009) 111-113.
28. G. Gupta, C. Lau, B. Branch, V. Rajendran, D. Ivnitski, P. Atanassov, *J. Electrochimica acta* 56 (2011) 10767-10771.
29. M. Togo, A. Takamura, T. Asai, H. Kaji, M. Nishizawa, *J. Power Sources* 178 (2008) 53-58.
30. T. Beneyton, I. P. M. Wijaya, C. Ben Salem, A. D. Griffiths, V. Taly, *J. Chem. Comm.* 49 (2013) 1094-1098.
31. A. Henni, A. Karar, *Materials and Biomaterials Science.* 01 (2018) 001-005.
32. A. Zebda, J. Renaud, M. Cretin, F. Pichot, C. Innocent, R. Ferrigno, S. Tingry, *J. Electrochem. Comm.* 11 (2009) 592-595.
33. T. Szabo, A. Szeri, I. Dékany, *J. Carbon* 43 (2005) 87-94.
34. H. Sakai, T. Nakagawa, Y. Tokita, T. Hatazawa, T. Ikeda, S. Tsujimura, K. Kano, *J. Energy & Environmental Science* 2 (2009) 133-138.
35. G. Li, J. Hao, *J. Electrochem. Soc.* 156 (2009) 134-138.
36. C. M. Moore, S. D. Minteer, R. S. Martin, *J. Lab Chip* 5 (2005) 218-225.
37. M. R. Thorson, F. R. Brushett, C. J. Timberg, P. J. A. Kenis, *J. Power Sources* 218 (2012) 28-33.
38. S. K. Yoon, G. W. Fichtl, P. J. A. Kenis, *J. Lab Chip* 6 (2006) 1516-1524.
39. A. Bazylak, D. Sinton, N. Djilali, *J. Power Sources* 143 (2005) 57-66.
40. A. E. Khabbazi, A. J. Richards, M. Hoorfar, *J. Power Sources* 195 (2010) 8141-8151.
41. S. Topcagic, S. D. Minteer, *J. Electrochimica Acta* 51(2006) 2168-2172.
42. D. Selloum, A. Abou Chaaya, M. Bechelany, V. Rouessac, P. Miele, S. Tingry, *J. Mater. Chem. A.* 2 (2014) 2794 -2800.
43. [43] L. Deng, L. Shang, D. Wen, J. Zhai, S. Dong, *J. Biosens. Bioelectron.* 26 (2010) 70-73.
44. S. A. Neto, J. C. Forti, V. Zucolotto, P. Ciancaglini, A. R. de Andrade, *J. Biosens. Bioelectron.* 26 (2011) 2922-2926.
45. D. E. Gutiérrez-Domínguez, D. E. Pacheco-Catalán, R. Patiño-Díaz, B. Canto-Canché, M. A. Smit, *J. Hydrogen Energy* 38 (2013) 12610-12616.
46. S. A. Neto, T. S. Almeida, L. M. Palma, S. D. Minteer, A. R. de Andrade, *J. Power Sources* 259 (2014) 25-32.

Acknowledgements

Financial supports by the ‘Hybiocell’ project in the framework of the ANR program International II and by the European Commission in the framework of an Averroes grant are gratefully acknowledged.

Conflicts of interest

Authors declare no conflict of interests.

Notes

The authors declare no competing financial interest.

Materials & Biomaterials Science

This is an open access article distributed under the terms of the Creative Commons Attribution License, which permits unrestricted use, distribution, and reproduction in any medium, provided the original author and source are credited.

How to cite this article

D. Selloum, S. Tingry, Ethanol /Oxygene microfluidic biofuel cells. *Mat. Biomater. Sci.* 01 (2018) 011-015.